A Short Review on Non-data-adaptive Multiscale Transforms Application to Atomic Representation of OCT Images

Raha Razavi*, Gerlind Plonka*, Hossein Rabbani†

1 Non-Data-Adaptive Transforms

The non-data-adaptive transforms are defined by fixed basis or frame functions and are commonly used for sparse representation applications. The Discrete Cosine Transform (DCT) [1] is able to present also periodic high-frequency data efficiently. Depending on the geometry of the image, the point singularities can be well detected by the tensor-product wavelet transform [2], edge singularities can be sparsely represented by the Dual-Tree Complex Wavelet Transform (DTCWT) [3], Wedgelets [4], Ridgelets [5], Curvelets [6], Shearlets [7], or the Ellipselets [8]. We will briefly summarize these so-called X-let transforms, and their advantages and drawbacks, in the next section.

1.1 Atomic Representation

In this section, we will discuss the decomposition of an OCT image using different non-data-adaptive transforms. The atomic representation of the image is obtained as a basis or frame representation, where all information of the image is then contained in the obtained basis or frame coefficients.

We briefly summarize the mentioned transforms chronologically in image processing applications in the following subsections.

1.1.1 Two-dimensional Discrete Cosine Transform (DCT)

The DCT has many applications in signal and image processing as image and audio compression, noise removal, high-performance scientific computing, derivative computation, and mainly frequency spectrum analysis, to mention a few [1], [9], [10]. Most of the time the so-called DCT-II is employed, but there exist also other DCT transforms, see The two-dimensional (2D) DCT is not an X-let transform. Differently from all other transforms that we will apply, the DCT is given here already as a transform that does not apply on functions but on discrete data, i.e., it maps from $\mathbb{R}^{N_1 \times N_2} \to \mathbb{R}^{N_1 \times N_2}$.

*Institute for Numerical and Applied Mathematics, Göttingen University, Lotzestr. 16-18, 37083 Göttingen, Germany. (emails: {plonka,r.razavi}@math.uni-goettingen.de)

†Medical Image and Signal Processing Research Center, School of Advanced Technologies in Medicine, Isfahan University of Medical Sciences, Isfahan, Iran. (email: h_rabbani@med.mui.ac.ir)

For a given discrete image $\mathbf{X} = (X_{k_1,k_2})_{k_1,k_2=0}^{N_1-1,N_2-1} \in \mathbb{R}^{N_1 \times N_2}$ the 2D-DCT maps $\mathbf{X}$ to $\hat{\mathbf{X}} = (\hat{X}_{n_1,n_2})_{n_1,n_2=0}^{N_1-1,N_2-1}$, and since it is an orthogonal transform, the inverse 2D DCT-II can be presented analogously,

$$\hat{X}_{n_1,n_2} = \varepsilon_{n_1}\varepsilon_{n_2} \sum_{k_1=0}^{N_1-1} \sum_{k_2=0}^{N_2-1} X_{k_1,k_2} \cos\left(\frac{\pi(2k_1+1)n_1}{2N_1}\right)$$
$$\cos\left(\frac{\pi(2k_2+1)n_2}{2N_2}\right), n_i = 0, \dots, N_i - 1, i = 1, 2.$$
$$X_{k_1,k_2} = \sum_{n_1=0}^{N_1-1} \sum_{n_2=0}^{N_2-1} \varepsilon_{n_1}\varepsilon_{n_2} \hat{X}_{n_1,n_2} \cos\left(\frac{\pi(2k_1+1)n_1}{2N_1}\right)$$
$$\cos\left(\frac{\pi(2k_2+1)n_2}{2N_2}\right), k_i = 0, \dots, N_i - 1, i = 1, 2.$$
$$\varepsilon_{n_\ell} := \begin{cases} \sqrt{\frac{1}{N_\ell}} & , 1 \le n_\ell \le N_\ell - 1 \\ \sqrt{\frac{2}{N_\ell}} & , n_\ell = 0 \end{cases}, \text{ for } \ell = 1, 2.$$

see e.g. [1, 11]. The 2D DCT-coefficients $\hat{X}_{n_1,n_2}$ of $\mathbf{X}$ provide information on the amplitudes of different frequencies appearing in $\mathbf{X}$. Applying 2D DCT on an image gives sparse representations of periodic texture as shown in many applications [9]. There are fast algorithms available with a complexity of $\mathcal{O}(N_1 N_2 \log(N_1 N_2))$, see e.g. [1, 11].

However, the application of the 2D DCT to the complete image $\mathbf{X}$ is not always favorable since the underlying cosine basis functions are not localized in space but periodic. Discontinuities in images that do not appear periodically lead to a slow decay of the DCT coefficients. To achieve localization in space, one can apply the 2D DCT to smaller image blocks or introduce the so-called short-time DCT, where we apply a convolution with a localized window function to $\mathbf{X}$ before applying the 2D-DCT.

1.1.2 Discrete Wavelet Transform (DWT) and Dual-Tree Complex Wavelet Transform (DT-CWT)

The desire for a new basis for signal analysis in $L^2(\mathbb{R})$ which is localized in space and in frequency led to a bunch of different constructions of wavelet bases, where the orthogonal Meyer wavelets with compact support in frequency (Fourier) domain, orthogonal Daubechies wavelets with compact support in the space domain, as well as biorthogonal spline wavelets, are the most used bases [2]. In the one-dimensional setting the wavelet bases are usually constructed using a so-called multiresolution analysis to obtain a (refinabe) scaling function ϕ with $\hat{\phi}(0) > 0$ and a mother wavelet function ψ with $\hat{\psi}(0) = 0$ (where $\hat{\phi}$ denotes the Fourier transform of ϕ). The mother wavelet function ψ can always be represented as a linear combination of $\phi(2 \cdot -k)$ for $k \in \mathbb{Z}$. A basis of $L^2(\mathbb{R})$ can be given by translation and dilation of one mother wavelet ψ, i.e., the basis is of the form $\{\psi_{j,k} = 2^{j/2}\psi(2^j \cdot -k) : j, k \in \mathbb{Z}\}$, such that any signal $f \in L^2(\mathbb{R})$ can be represented as

$$f = \sum_{j \in \mathbb{Z}} \sum_{k \in \mathbb{Z}} \left\langle f, \tilde{\psi}_{j,k} \right\rangle_{L^2} \psi_{j,k}.$$

where $\tilde{\psi}_{j,k} = \psi_{j,k}$, if the wavelet basis is orthogonal, otherwise $\tilde{\psi}_{j,k}$ denotes the dual (biorthogonal) wavelet function. Here $\left\langle f, \tilde{\psi}_{j,k} \right\rangle_{L^2}$ are called wavelet coefficients, which

decay quickly, if f is (locally) smooth. There are fast algorithms available for the discrete wavelet transform, which can be conducted using a so-called wavelet filter bank consisting of convolution and down-sampling operators. The fast discrete wavelet transform can be extended to the two-dimensional case by a tensor product approach.

However, there are several drawbacks of the DWT that were pointed out in the literature [3]. In the first place is the missing shift invariance property. Wavelet coefficients are highly sensitive to small shifts in the data which causes apparent artifacts in the reconstructed image. Further, around the point or edge singularities, several large wavelet coefficients appear with changing signs. Iterated discrete-time downsampling and passing through low-pass and high-pass filters are the main steps of computing the wavelet coefficients and the major reason for aliasing effects. Performing any signal or image processing operation such as thresholding, filtering, or quantization of the coefficients unbalances the relationship between the forward and inverse transforms and causes artifacts in the outcome. Finally, the simple tensor product DWT covers only four main directions well, see Fig. 1b, i.e., it is not rotationally invariant, which is a disadvantage for modeling the geometrical features in an image.

To overcome the mentioned problems of the wavelet transform, the Complex Wavelet Transform (CWT) has been introduced in [3]. The CWT is based on a complex-valued scaling function $\phi = \phi_1 + i\,\phi_2$ and a complex wavelet function $\psi = \psi_1 + i\psi_2$. These functions are constructed such that the imaginary part ψ_2 is approximately the Hilbert transform of ψ_1 to achieve an approximatively analytic signal ψ. As a complex function, ψ can be also rewritten as $\psi(t) = A(t)\,\mathrm{e}^{\mathrm{i}\varphi(t)}$ with the non-negative envelope function $A(t)$ and the phase function $\varphi(t)$. The obtained complex wavelet dictionary is no longer a basis but a (tight) frame for $L^2(\mathbb{R})$ with redundancy factor 2.

The discrete Dual-Tree CWT (DTCWT) employs two (real) wavelet filter banks, one for the real part and one for the imaginary part, where the filters of each of these filter banks are designed such that the overall transform is approximately analytic. This transform can also be extended to the two-dimensional case, see [3]. The transform then achieves nearly shift invariance and nearly rotation invariance supporting sparse detection of eight directions. Fig. 1b illustrates the difference between the directionality selectivity of DTCWT and DWT in the frequency plane.

1.1.3 Ridgelet Transform and Curvelet Transform

The missing rotation invariance of the tensor-product wavelet approach motivated further more sophisticated multi-scale frame constructions. To detect the straight-line singularities, the theory of Ridgelets was proposed [5]. Systems of bivariate Ridgelet functions use translations, dilations, and rotations of one function ψ and are of the form

$$\psi_{a,b,\theta}(x_1, x_2) = a^{-1/2}\psi((x_1\cos(\theta) + x_2\sin(\theta) - b)/a),$$

where ψ is a smooth localized function with $\int_{\mathbb{R}} |\hat{\psi}(\omega)|^2/\omega^2 d\omega < \infty$. Here a denotes the scale, b the position, and θ the rotation angle. In particular, the rigdelet function $\psi_{a,b,\theta}$ is constant along lines $x_1\cos\theta + x_2\sin\theta = \text{const}$. Fast implementations of the discrete ridgelet transform employ the fast discrete NFFT-based Radon and translation-invariant discrete Wavelet transform, see e.g. [12]. Fig. 1d represents the frequency domain partition of the Ridgelet transform.

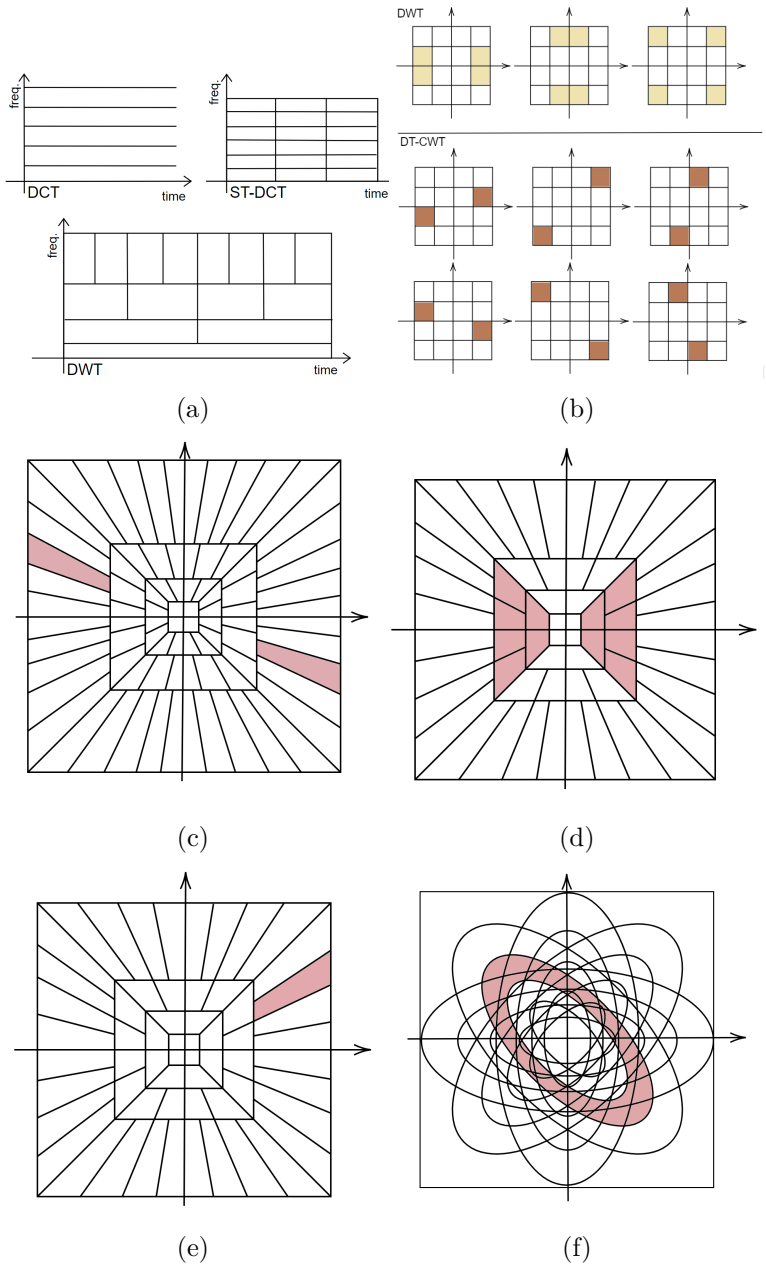

Figure 1: (A) DCT, ST-DCT, and DWT tiling in the frequency domain. (B) Directionality DWT and DT-CWT. The tiling of the (C) Shearlet, (D) Ridgelet, (E) Curvelet, and (F) Ellipselet transforms in the frequency domain.

Ridgelets are also called first-generation Curvelets. The system of Curvelets was introduced [6] to detect not only line singularities but also curve singularities. The Curvelet frame also consists of functions which are obtained by translation and rotation of one basic dilated Curvelet function ψ, and the atoms of the Curvelet frame smoothly approximate the characteristic functions of wedges in the frequency domain, see Fig. 1e. Suitable Curvelet basis functions are well-localized in the space and frequency domain and this results in high directional selectivity. This over-complete system of atoms allows a sparse representation of piecewise smooth image functions with edge singularities along smooth curves [6]. However, for curve singularities with less smoothness, the Curvelet represen-

tations are no longer optimal. The discrete Curvelet transform often uses a pseudo-polar grid in the frequency domain, see e.g. [13, 14].

1.1.4 Shearlet Transform

Another non-data-adaptive transform is the Shearlet transform [7, 18]. A (regular) discrete Shearlet function system consists of functions of the form,

$$\psi_{j,k,m} = 2^{3j/4}\psi\left(S_k A_{2^j} \cdot - m\right), \quad j,k \in \mathbb{Z}, m \in \mathbb{Z}^2$$
$$\text{with} \quad A_{2^j} = \begin{pmatrix} 2^j & 0 \\ 0 & 2^{j/2} \end{pmatrix},\ S_k = \begin{pmatrix} 1 & k \\ 0 & 1 \end{pmatrix},$$

where ψ is a tensor product of one-dimensional Wavelet functions, A_{2^j} is a dilation matrix, and S_k is a shear matrix. The Shearlet frame has some similarities to the Curvelet system but has different algebraic structures. It is possible to construct a tight Shearlet frame for $L^2(\mathbb{R}^2)$ in the well-chosen discrete setting [18]. There are different Shearlet constructions available, in particular constructions with compactly supported frame functions either in the frequency domain or in the space domain. Although the Shearlet decomposition provides an acceptable sparse representation, the reconstruction results usually have artifacts around sharp discontinuities. The frequency tiling of the Shearlet transform is presented in Fig. 1c. For algorithms for the discrete Shearlet transform we refer to [18, 17, 16].

1.1.5 Ellipselet Transform

The Circlet transform is based on a frame of atoms with essential support on circular rings with different radii, which can be shifted in $\mathbb{R}^2$ [19]. In the frequency domain, the frame atoms are constructed in polar coordinates as a product of a one-dimensional band-pass function (Wavelet), that depends only on the radius, and a modulation factor depending on the angle. Generalizing this idea, another frame has been introduced in [8], where frame atoms with elliptical shapes in the frequency domain have been introduced to optimally detect objects having an ellipse, circle, or curved shape. The Ellipselet construction uses a specific norm to achieve the elliptic shape of the frame atoms. Tilling of the frequency domain of the Ellipselet transform with four basis functions (at angles $0°$, $90°$, $-45°$, and $45°$) is shown in Fig. 1f. The results show that curves are preserving well but not the background texture area since the selected oscillating function such as wavelet is involved.

The different frequency tilings given in Figure 1 show how the partition of the frequency domain is achieved in different ways by the considered non-adaptive transforms. We conclude that each of the non-data-adaptive transforms may present some specific data in a sparse way, yet, may perform poorly for other types of data. Since the basis or frame functions are a prior defined, the result is highly dependent on the geometrical characteristics of the input image. Therefore, selecting the more appropriate transforms and combining them may lead to a better denoising performance.

Among the above transforms, DCT presents the texture of OCT images the best. DT-CWT presents the non-texture parts specifically the layers the best. The Curvelet

transform well represents the line and curves singularities (the layers in the OCT images). The Ellipselet transform behaves consistently for different types of OCT images and presents the singularities sufficiently well but not the texture area. Hence, the basis or frame functions corresponding to these four transforms will be used to be our representative atom selections for OCT images. Since each of these transforms serves a purpose, one is well suited for capturing the texture but not the non-texture parts, and the other reverse, we are interested in designing a redundant dictionary that includes the DCT, DTCWT, Curvelet, and Ellipselet atoms. In [20] and [21], we focused on exploiting the advantages of these transforms in one redundant transform. We showed the application of this redundant transform in denoising of OCT images.

References

[1] N. Ahmed, T. Natarajan, K.R. Rao, "Discrete Cosine Transform," *IEEE Trans. Comput.*, vol. C-23, n. 1, pp. 90-93, 1974.

[2] S. Mallat, "A wavelet tour of signal processing: the sparse way, third edition," *Academic Press*, 2009.

[3] I. W. Selesnick, R. G. Baraniuk, N. G. Kingsbury, "The Dual-Tree Complex Wavelet Transform," *IEEE Signal Process. Mag.*, vol. 22, pp. 123-151, 2005.

[4] V. Kiani, A. Harati, A. Vahedian Mazloum, "Iterative Wedgelet Transform: An efficient algorithm for computing Wedgelet representation and approximation of images," *J. Vis. Commun. Image Represent.*, vol. 34, pp. 65–77, 2016.

[5] E. J. Candès, "Ridgelet: Theory and applications," Ph.D. thesis, Department of Statistics, Stanford University, 1998.

[6] E. J. Candès, D. L. Donoho, "New tight frames of curvelets and optimal representations of objects with piecewise-C^2 singularities," *Comm. on Pure and Appl. Math.*, vol. 57, pp. 219–266, 2004.

[7] K. Guo, G. Kutyniok, D. Labate, "Sparse Multidimensional Representations using Anisotropic Dilation and Shear Operators," *J. Wavelets and Splines*, May 2005.

[8] Z. Khodabandeh, H. Rabbani, A. Mehri Dehnavi and O. Sarrafzadeh, "The Ellipselet Transform," *J. Med. Signals Sens.*, vol. 9, pp. 145–157, Sep. 2019.

[9] K. R. Rao, P. Yip, "Discrete Cosine Transform: Algorithms, Advantages, Applications," *Elsevier Science & Technology Books*, Chapter 7, Application of the DCT, pp. 136-348, 1990.

[10] G. Yu, G. Sapiro, "DCT Image Denoising: a Simple and Effective Image Denoising Algorithm," *Image Process. On Line*, vol. 41, pp. 292–296, 2011.

[11] G. Plonka, D. Potts, G. Steidl, M. Tasche, "Numerical Fourier Analysis", *Birkhäuser*, 2018.

[12] M. Fenn and J. Ma, "Combined complex ridgelet shrinkage and total variation minimization", *SIAM J. Sci. Comput.* vol. 28, pp. 984-1000, 2006.

[13] E. Candes, L. Demanet D. Donoho L. Ying, "Fast discrete curvelet transforms", *Multiscale Modeling & Simulation*, vol. 5(3), pp. 861-899, 2006.

[14] J. Ma, G. Plonka, "A Review of Curvelets and Recent Applications", *IEEE Signal Process. Mag.*, vol. 27, pp. 118-133, 2010.

[15] P. Kittipoom G. Kutyniok, and W.-Q Lim, "Construction of compactly supported shearlet frames", *Constructive Approximation*, vol. 35 (1), pp. 21-72, 2012.

[16] K. Guo and D. Labate, "The construction of smooth Parseval frames of shearlets", *Math. Model. Nat. Phenom.*, pp. 82-105, 2013.

[17] S. Häuser and G. Steidl, "Fast Finite Shearlet Transform: a tutorial", arXiv:1202.1773, 2014.

[18] D. Labate, W.-Q. Lim, G. Kutyniok, G. Weiss, "Sparse multidimensional representation using shearlets,"*Proc. SPIE Wavelets XI*, vol. 5914, pp. 254–262, 2005.

[19] H. Chauris, I. Karoui, P. Garreau, H. Wackernagel, P. Craneguy, and L. Bertino, "The circlet transform: A robust tool for detecting features with circular shapes", *Comput. Geosci.*, vol. 37, pp. 331-342, 2011.

[20] R. Razavi, G. Plonka, H. Rabbani, "X-let's atom combinations for modeling of OCT images by modified morphological component analysis", , University of Goettingen, 2023.

[21] R. Razavi, H. Rabbani, G. Plonka, "Combining non-data-adaptive transforms for OCT image denoising by iterative basis pursuit,"*IEEE Int. Conf. Image Process. (ICIP)*, pp. 2351-2355, 2022, doi: 10.1109/ICIP46576.2022.9897319.